IASSNS-AST-93-6B

Hubble Space Telescope Observations of the Center of Globular Cluster M15[1]

BRIAN YANNY

Institute for Advanced Study, Princeton NJ 08540

yanny@guinness.ias.edu

P. GUHATHAKURTA

Princeton University, Princeton NJ 08540 Princeton U.

D. P. SCHNEIDER, J. N. BAHCALL

Institute for Advanced Study, Princeton NJ 08540

Princeton, Inst. Advanced Study

IASSNS-AST-93-6B

Fermilab Library
0 1160 0020156 0

ABSTRACT

Images of the dense center of globular cluster M 15 (NGC 7078) have been obtained with the Hubble Space Telescope in the V and I filters. Accurate photometry is possible in the very densest part of the cluster center with rms errors of < 0.3 magnitudes for stars down to the main sequence turnoff. Evidence for radial segregation between horizontal branch, red giant branch, and blue straggler stars is presented. We discuss the possibility of the existence of a central stellar density cusp which does not flatten into a small central core at radii less than 2 arcseconds.

[1]Based on observations with the NASA/ESA Hubble Space Telescope obtained at the Space Telescope Science Institute, which is operated by the Association of Universities for Research in Astronomy, Inc., under NASA contract NAS5-26555

1. INTRODUCTION

The globular cluster M15 has one of the highest central projected stellar densities of all known clusters. Within the central arcsecond ($1'' = 0.062$ pc), the projected stellar density for stars with $V < 19$ (above the main sequence turnoff) is greater than 5000 stars pc^{-2}. Only one or two other known globular cluster have central densities this high. One would like to know if this high stellar density has had in the past an effect on the stellar populations in the cluster and how the high density affects the dynamical evolution of stars in the cluster (see Hut et al 1992 for a review).

A more extensive treatment of this work may be found in Yanny et al (1993).

2. Observations and Reductions with Simulations

Hubble Space Telescope (HST) observations of the center of M15 were obtained with the Planetary Camera (PC) in the F555W (V band, 3 exposures total) and F785LP (I band, 2 exposures total) filters on 10 December 1990 and 11 April 1991. Exposure times ranged from 70 to 300 seconds in length. Additionally, we have reprocessed four 800 second exposures of the cluster taken with the HST/PC through the F336W (U) filter, previously analyzed by Lauer et al (1991).

The spherical aberration of the HST optics results in a spatially varying PSF that has a sharp FWHM= $0''.1$ core and a diffuse $r = 2''.5$ halo, thus faint stars sitting in the $2''.5$ wings of bright stars are accurately fit only if the point spread function (PSF) model very accurately subtracts off the wings of the bright star. Additionally, the 12-bit resolution of the A/D converters in the HST/PC camera CCD electronics restricts the dynamic range available between brightest and dimmest magnitudes, resulting in saturation of the brightest stars. We have developed a procedure based on DAOPHOT (Stetson 1987) for modeling the HST/PC PSF as it varies across the 4 CCD $68'' \times 68''$ mosaic and for correcting for saturated bright stars. This procedure is detailed in Guhathakurta et al (1992), hearafter Paper I.

To determine completeness and photometric accuracy of the PSF fitting technique, extensive simulations have been run. The simulations proceeded as follows: An approximate luminosity function was derived from star counts as a function of magnitude in less crowed

regions of M15. At faint magnitudes this luminosity function was extended as shown in Figure 1.

Then stars were randomly drawn from a radial distribution having either 1) a central density cusp with $\alpha = -0.75, N(r) \sim r^{\alpha}$; or 2) a small flat $r_c = 2''$ King-model core $N(r) \sim 1/(1 + (r/r_c)^2)$, where $N(r)$ is the projected (surface) stellar density. These stars were assigned randomly a magnitude drawn from the luminosity function described above and placed on the simulated image with a PSF similar to the "true HST" PSF (see Paper I). The number of stars was normalized so that the bright star counts accurately matched those seen in M15. The sum of the light from all the faint stars in the simulated image was intended to reproduce the faint diffuse light seen in M15 after the bright stars had been subtracted.

The bright stars in the simulated images were truncated to represent saturation and the images were reduced as one would reduce any real data image, without knowledge of positions or magnitudes of the stars and without knowledge of the PSF used to create the simulated image.

Photometric accuracy as determined by the simulations is presented in Figure 2. It is seen that accuracy of $1\sigma < 0.15$ mag is obtained for $V < 16$ and $1\sigma \sim 0.3$ mag is obtained for stars with $V < 19$, above the main sequence turnoff. A goal of these simulations is to determine whether, following the work of Cohn (1993), one can decide if the projected stellar density in the central $2''$ of M15 resembles a central cusp with some power law profile into $r < 1''$ or more closely matches a flat "King-model" core of some finite and resolved core radius. The implication of the cusp profile with power-law slope $\alpha = -0.75$ is that the cluster has undergone core collapse and may contain a massive black hole in its core (Bahcall and Wolf 1976, 1977). A power law cusp profile does not necessarily imply the existence of a central compact object. Models of run away core collapse in a cluster without formation of a black hole suggest a slope of something like $\alpha = -1.4$ (Heggie 1985). Observations of a flat King-model core of finite radius $r \gtrsim 0.05$ pc suggests binary heating has halted or reversed the collapse (Hut et al 1992).

From the simulations one can determine the usefulness of analyzing the diffuse "residual" light which remains on the simulations after the bright stars have been subtracted using the PSF-fitting procedure. We show in Figures 3 and 4 the residual radial profile of the light which remains after subtraction of bright stars ($V < 18$) plotted against the initial summed light of all faint stars with ($V > 19$). The residual light is the sum of poorly subtracted bright star residuals and that of unresolved faint stars. The two curves should follow one another and have the same shape if the subtraction of the bright stars is done in the same way systematically as a function of radius. In the cusp simulation of Figure 4 it is clear that that this is not the case. The "flat core" seen in residual light does not closely follow the initial radial distribution of stars and is, in fact, an artifact of the reduction process. Thus, if a steep power-law cusp existed for the star light in the actual real data, that cusp would not become apparent by examining the profile of residual diffuse light. The residual light is not a good cusp/core discriminant; actual star counts of resolved stars must be used.

We note that a King model with $r_c \sim 2''$ core is not necessarily the most likely fit to the projected radial profile of the cluster M15 (Lauer et al 1991).

Why does the reduction procedure tend to flatten out the core in regions of quickly varying sky brightness? Besides the fact that the HST/PC point spread function is broader than $r = 2''$, we believe there is a built-in bias in the PSF fitting program which tends to favor a "flat sky". In regions of rapid sky variation, excess sky light is absorbed into the wings of fainter stars, resulting in a systematically brighter stellar magnitude for a group of stars near the center of a region of high sky level derivative. This can be seen as a systematic positive (input - output) magnitude offset in Figure 2 for stars with $V > 16$.

3. Radial Profile

We present in Figure 5 the V stellar number counts (with $\sqrt{N}$ Poisson error bars) as a function of radius. One immediately notes that a flat core is not apparent to $r < 1''.5$ and in fact a fit to the data is consistent with a power law cusp of slope $\alpha < -0.75 \pm 0.1$. When corrected for incompleteness (which is a factor of 2 or more for $r < 2''$) this slope becomes even steeper. The data are also consistent with a King profile flat core of radius $\sim 1''.45$. We find the radial distribution of stars consistent with a number of scenarios, including 1) a

central black hole of mass > 1000$M_\odot$ (Peterson, Seitzer, and Cudworth 1989), 2) a collapsed core with steep central profile ($\alpha < -0.75$) and no black hole, or 3) a small flat core of radius $\lesssim$ 0.09 pc.

4. Color Segregation

A (V-I,V) color magnitude diagram (CMD) for the central 13″ of M15 is presented in Figure 6. Stars were included in the figure if they were detected in each of two independent V and I exposures and the magnitude variation between the two exposures of the same color is less than 0.5 mag. A significant blue horizontal branch (BHB) population is seen (Buonanno et al 1985) in addition to the regular horizontal branch (HB). A large population of about 30 blue stragglers occupies the region of the diagram below the HB and to the right and below the BHB. The 'flat top' effect seen at the bright end of the red giant branch, due to a deficit of very bright red giants in the core has been previously noted by Stetson (1991).

To quantify to effects of radial segregation in the core of the cluster, we separate the stellar populations into 4 types: red giant branch (RGB), HB, BHB, and blue straggler (BS) stars. The separation is based on I and F336W (approximately U band) magnitude with the following arbitrary separation definitions: RGB: ($U < 18.0$ and $U - I > 1.8$), HB: ($16 < U < 17.4$ and $U > 16$ and $U - I < 1.8$ and $U - I > 0.5$), BHB: ($U - I < 0.5$ and $16 < U < 17.4$), and BS: $17.4 < U < 18.6$ and $U - I < 0.7$. The result of these separations by type is shown in Figure 7. The separation is not ideal and there is certainly ambiguity between the BHB and BS regions.

In spite of the ambiguity, we proceed to plot a cumulative radial distribution in Figure 8 for the 4 types of stars and note the following:

First, the HB (red horizontal branch) appears to be significantly more centrally concentrated than the RGB. A Kolmorgorov-Smirnov (KS) test finds the effect significant at the 95% confidence level. This may be due to one of two effects (or a combination of both); either RGBs are depleted in the center or HBs are in excess. If we normalize star counts in annuli extending out from the center so that each annulus contains an equal number of stars with $16.5 < V < 17.5$ we find that the number of RGB stars is depleted in the central $r < 4''$

relative to the region with $4'' < r < 11''$. We are, however, in at least qualitative agreement with Bailyn et al (1988) in that there is not a strong trend of bluing with decreasing radius in the central $r < 11''$ of M15. The depletion of RGB stars is nearly matched by a deficit of BHB stars (see Stetson 1991 for a detailed discussion).

Second, the blue straggler stars, while they may be slightly centrally concentrated, are no where as nearly as concentrated as they are in, for instance the cluster 47 Tuc (Paper I), the significance of the central concentration from Figure 8, is only at about the 90% confidence level as indicated by a two-sided KS test vs the RGB stars. We offer the caveat that this small concentration is noted for the very center of the cluster ($r < 10''$) relative to the annulus with $10'' < r < 60''$ and in fact the lack of blue stragglers in the outer parts of the cluster ($r > 2'$) (Buonanno et al 1985; Sandage 1970), relative to the 30 or more found in the central arcminute appears to be significant. This suggests that on a larger scale, r$\sim 1'$, the BS are concentrated.

5. Summary

1. Images obtained in the F555W (V) and F785LP (I) filters are used to derive accurate photometry, $1\sigma = 0.15$ mag, of the stars above $V = 16$ and $1\sigma \sim 0.3$ mag above the main sequence turnoff (V$\sim$ 19).

2. The projected radial profile of stars within the central $5''$ of the cluster is consistent with a power law cusp of slope -0.75 ± 0.1 (and after completeness correction even steeper), consistent with a black hole and the velocity data of Peterson, Seitzer and Cudworth (1989).

3. The data are also consistent with a small core of radius less than $1''.5$, significantly smaller than the radius found by Lauer et al (1991). The difference is due to interpretation of the residual diffuse light in the core after stars are subtracted. We find that, given the broad HST PSF, residual light is unreliable in determining presence or absence of a core in regions of such high stellar density.

4. Evidence of earlier reports of little color segregation in the center of the cluster is confirmed in the sense that red giants are depleted in the center of the cluster relative to the sub-giants, but the depletion of very blue BHB stars counteracts this bluing trend in the

central 11″ of the cluster.

5. Numerous (at least 30) blue straggler stars are present in the center ($r < 60''$) of the cluster and only appear slightly concentrated in the inner 10″ compared to the next 50″.

We are grateful for the hospitality of STSCI where a version of this paper was presented as part of the Hubble Fellow Symposium on Nov 10, 1992. BY was supported by Hubble Fellowship HF-1013.01-90A.

Figure Captions

1. The open squares represent the actual star counts as a function of magnitude for stars with $4''.3 < r < 30''$ where completeness is assumed to be about 100% for $V < 18$. The black circles represent the extrapolated luminosity function used in the simulations to represent both bright and faint stars. The faint stars ($V < 19$) sum to a core or unresolved cusp of light.

2. Root mean square input vs input - output magnitudes for the photometric accuracy simulation. Errors of 0.15 magnitude are obtained for $V < 16$ and errors remain $\lesssim 0.3$ mag for stars above the M15 main sequence turnoff at $V \sim 19$. Note the slight systematic positive zero point offset for stars fainter than $V = 16$. This is due to the crowding in the central regions which tends to flatten the background "sky" level by adding extra light to numerous stars, systematically decreasing (brightening) their "output" magnitudes.

3. Input and residual diffuse light plot for King input profile simulation. The input diffuse light consists of the sum of light from all stars with $V > 18.5$, the residual diffuse light is all light that remains after subtraction of all modeled bright stars with $V < 18.5$.

4. Same as Figure 2 for cusp profile simulation. Note that the cusp disappears in the residual light leaving what appears to be a King profile of core radius about $4''$. This "false flat core effect" remains even after deconvolution of the diffuse light with a suitable HST point spread function.

5. Radial plot of V number counts of all stars with ($V < 18$) in the center of M15. Note that a flat core is not apparent, and the data are well fit by a power law of slope $\alpha < -0.75$.

6. (V-I,V) Color magnitude diagram for selected stars in the central $r < 13''$ of M15. These stars have accurate magnitudes in the sense that the variation in magnitude between two V and I exposures is less than 0.5 mag.

7. (U-I,V) Color magnitude diagram with the largest color baseline (U-I) and independent (x,y) axes so that correlated errors are not present. Selected subgroups of stars, namely red giant branch (RGB), (red) horizontal branch (HB), blue horizontal branch (BHB) and

blue stragglers (BS) are marked separately.

8. Cumulative radial distribution of stars of selected types in the core of M15. The HB stars are centrally concentrated with respect to the RGB stars, and within 10 arcsec, the BS stars are slightly centrally concentrated with respect to the RGB stars.

REFERENCES

Bahcall, J. N., & Wolf, R. A. 1976, ApJ, 209, 214

Bahcall, J. N., & Wolf, R. A. 1977, ApJ, 216, 883

Bailyn, C. D., Grindlay, J. E., Cohn, H., & Lugger, P. M. 1988, ApJ, 331, 303

Buonanno, R., Corsi, C. E., & Fusi Pecci, F. 1985, A&A, 145, 97

Cohn, H. 1993, private communication

Guhathakurta, P., Yanny, B., Schneider, D. P. & Bahcall, J. N. 1992, AJ 104, 1790 (Paper I).

Heggie, D. 1985 in "IAU #113 Dynamics of Star Clusters" eds Goodman, J., and Hut, P. p 139

Hut, P., et al 1992, PASP 104, 981

Lauer, T. R. et al 1991, ApJL, 369, L45

Peterson, R. C., Seitzer, P., & Cudworth, K. M. 1989, ApJ, 347, 251

Sandage A., 1970 ApJ 162, 841

Stetson, P. B. 1987, PASP, 99, 191

Stetson P. B., 1991, in "Precision Photometry" eds A G Davis Philip, A R Upgren & K A Janes 1991, p 69

Yanny, B., Guhathakurta, P., Schneider, D. P. & Bahcall, J. N. 1993, AJ in preparation

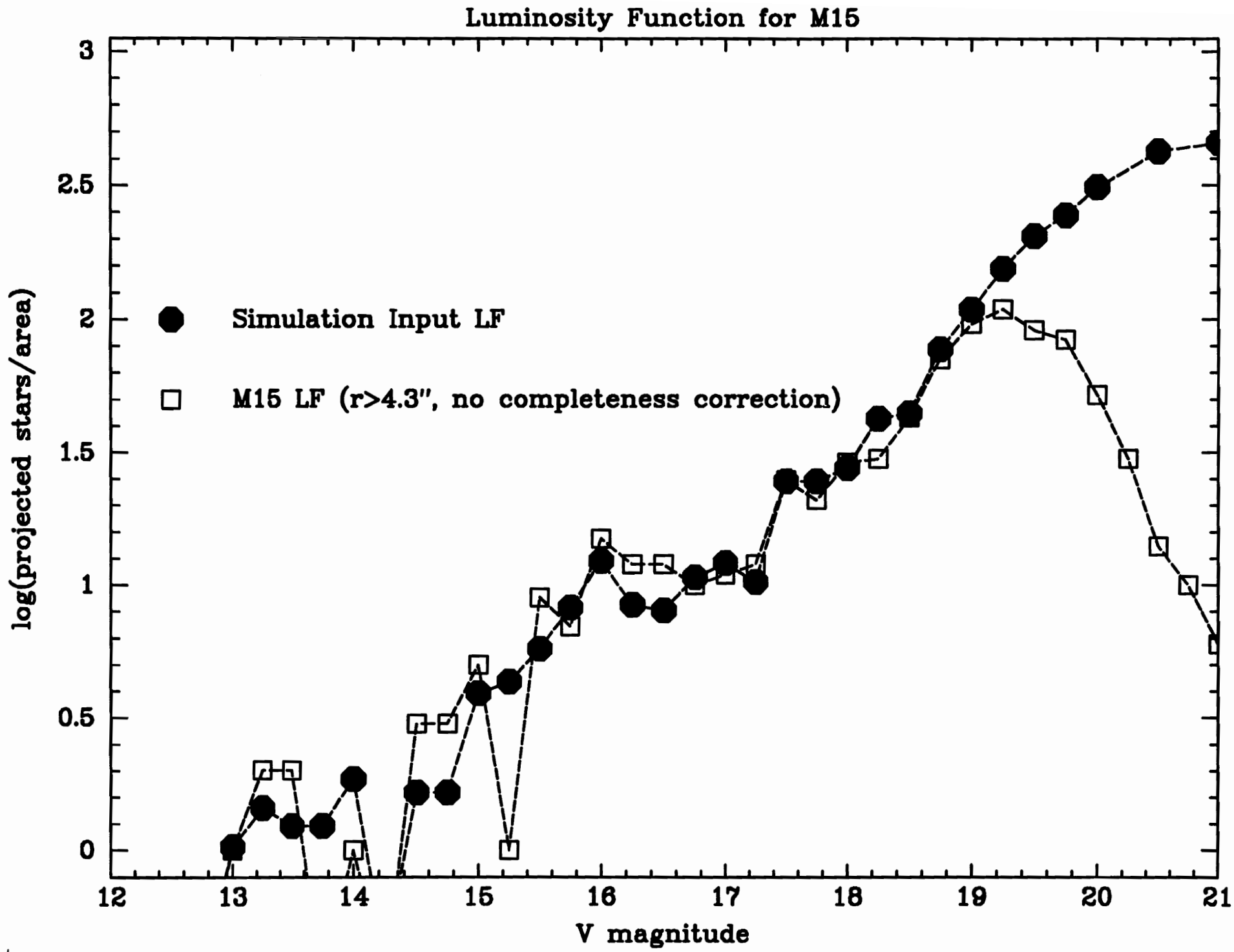
Luminosity Function for M15
Simulation Input LF
M15 LF (r>4.3", no completeness correction)
log(projected stars/area)
V magnitude
3
2.5
2
1.5
1
0.5
0
12
13
14
15
16
17
18
19
20
21

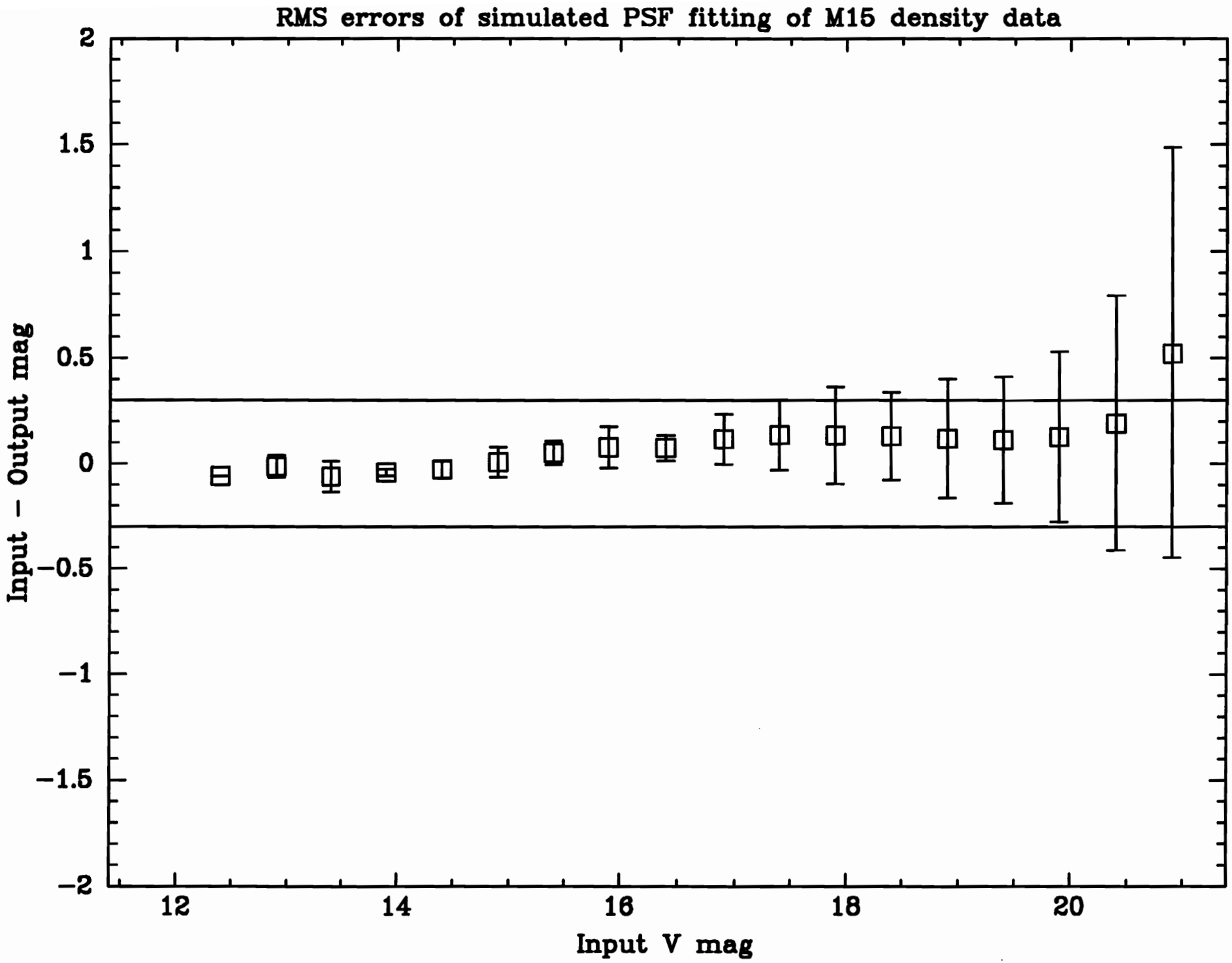
RMS errors of simulated PSF fitting of M15 density data
Input − Output mag
Input V mag
2
1.5
1
0.5
0
−0.5
−1
−1.5
−2
12
14
16
18
20

2

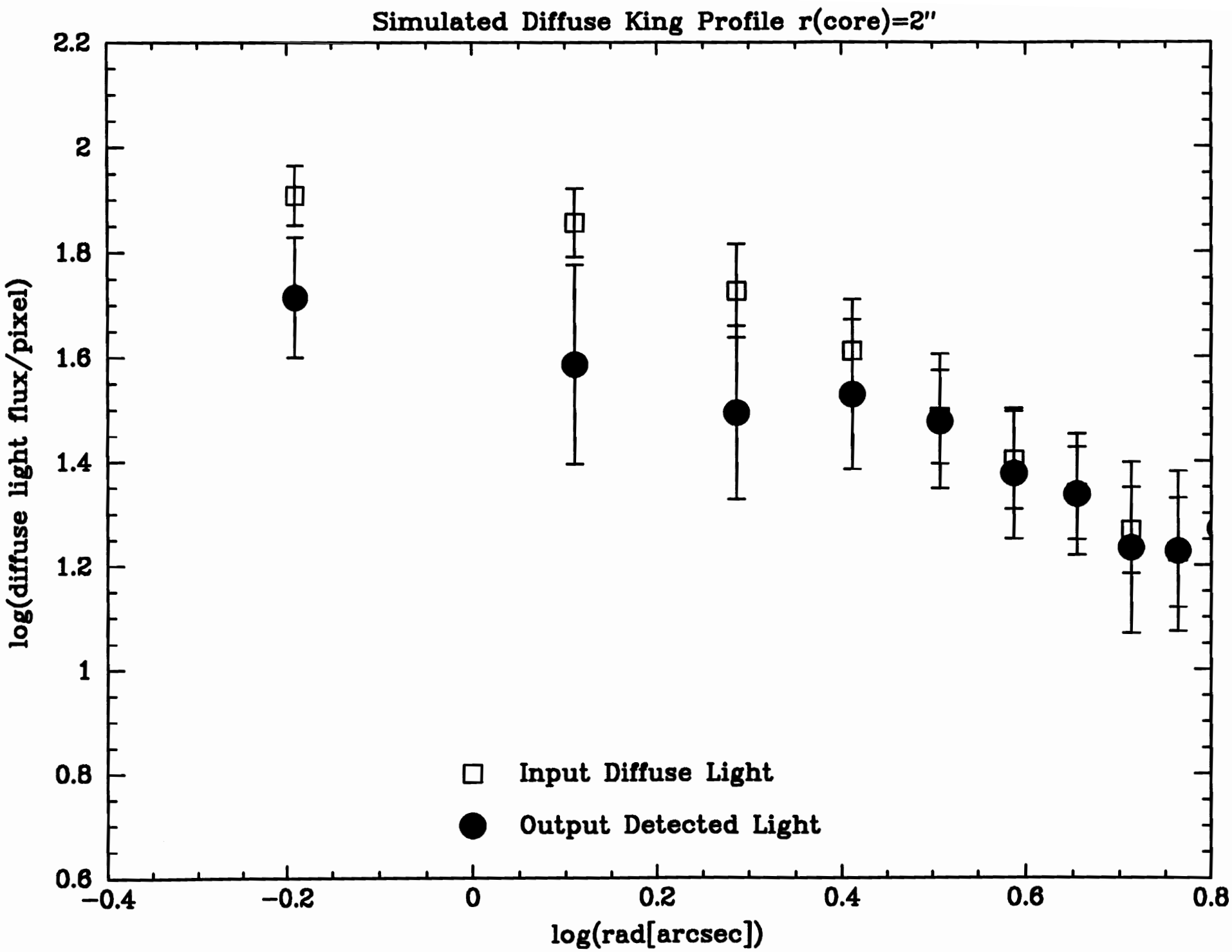
Simulated Diffuse King Profile r(core)=2"
log(diffuse light flux/pixel)
log(rad[arcsec])
Input Diffuse Light
Output Detected Light
2.2
2
1.8
1.6
1.4
1.2
1
0.8
0.6
−0.4
−0.2
0
0.2
0.4
0.6
0.8

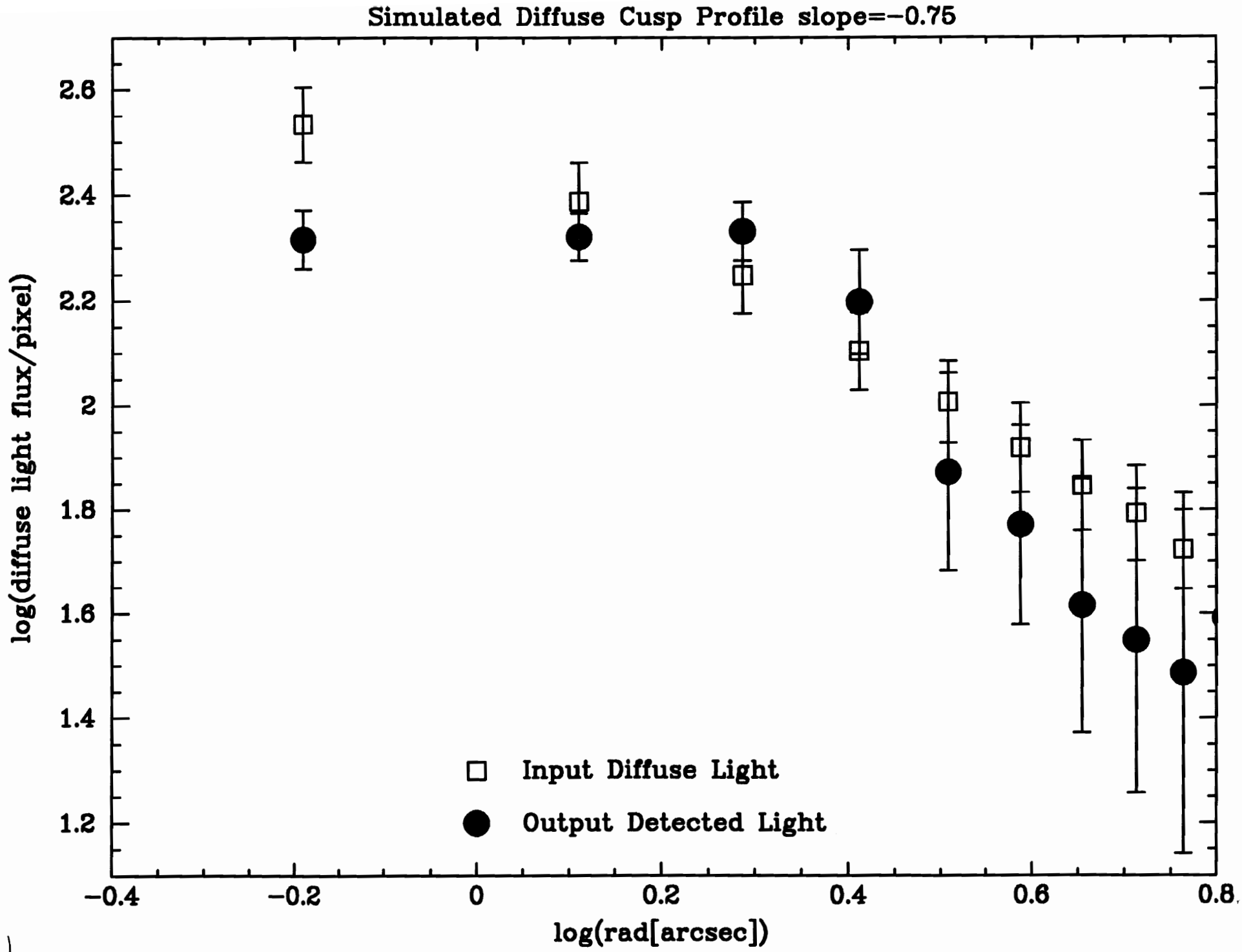
Simulated Diffuse Cusp Profile slope=−0.75
log(diffuse light flux/pixel)
2.6
2.4
2.2
2
1.8
1.6
1.4
1.2
−0.4
−0.2
0
0.2
0.4
0.6
0.8
log(rad[arcsec])
Input Diffuse Light
Output Detected Light

4

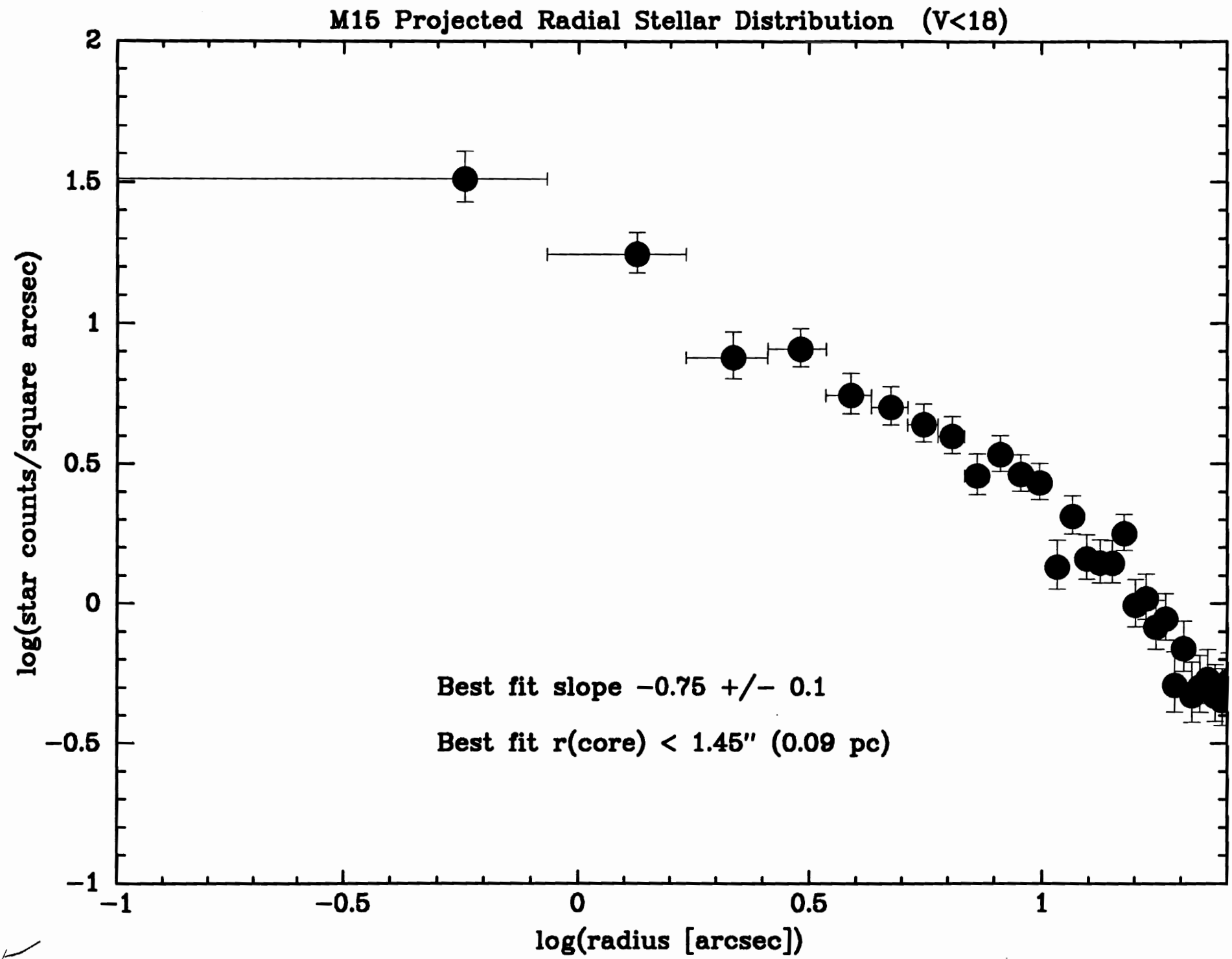
M15 Projected Radial Stellar Distribution (V<18)
log(star counts/square arcsec)
log(radius [arcsec])
Best fit slope −0.75 +/− 0.1
Best fit r(core) < 1.45″ (0.09 pc)
2
1.5
1
0.5
0
−0.5
−1
−1
−0.5
0
0.5
1

5

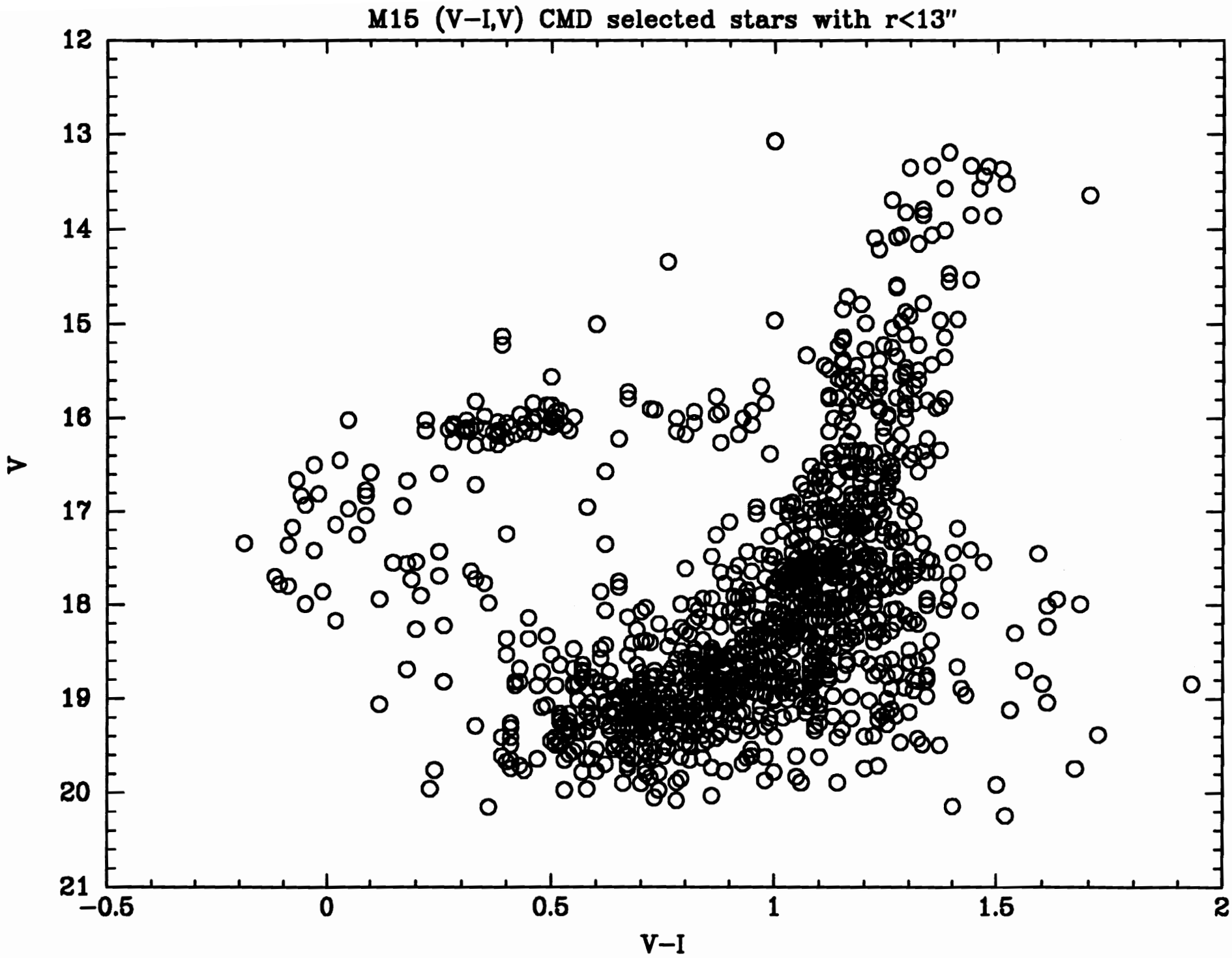
M15 (V−I,V) CMD selected stars with r<13"
V
V−I
12
13
14
15
16
17
18
19
20
21
−0.5
0
0.5
1
1.5
2

6

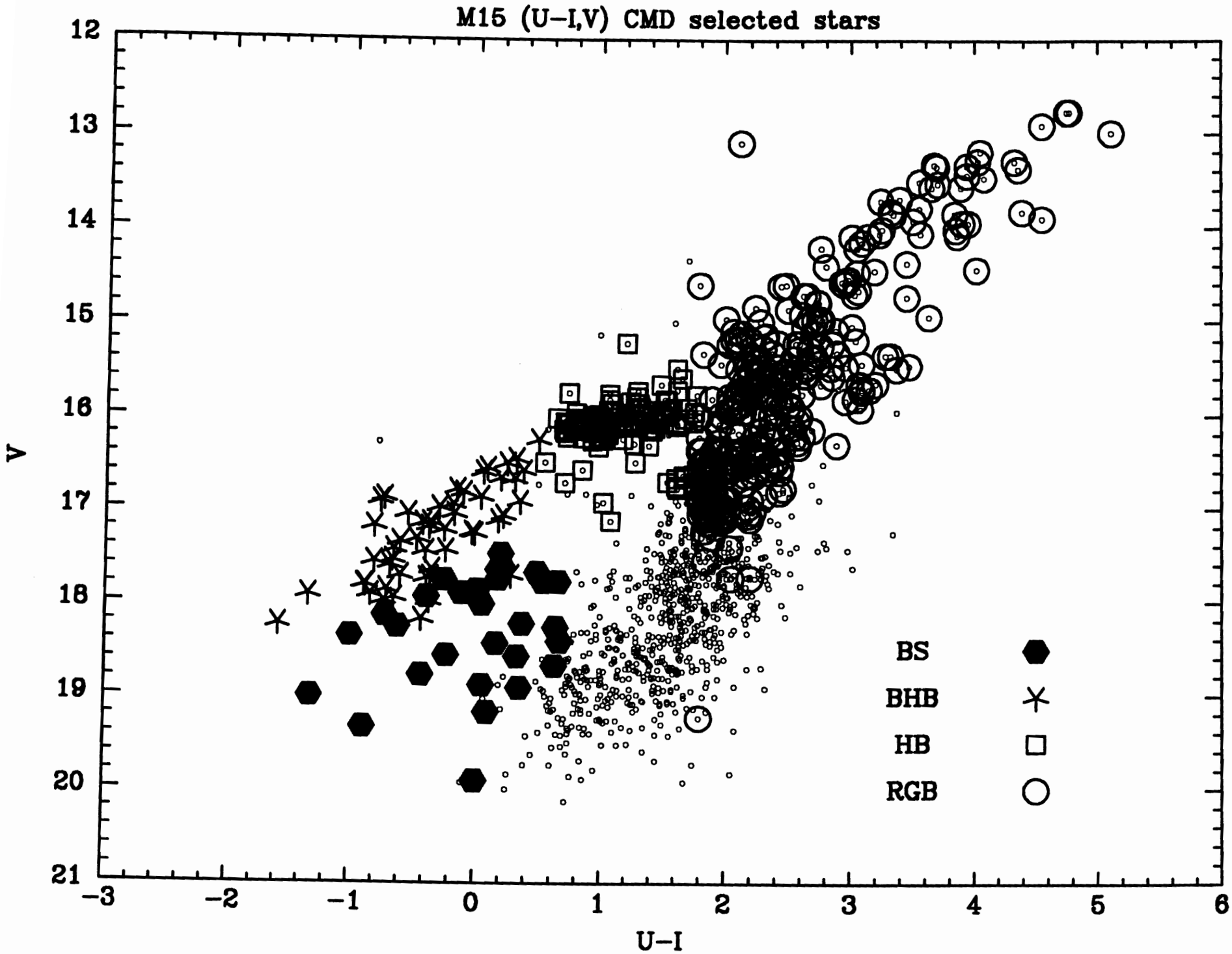
M15 (U−I,V) CMD selected stars
V
U−I
12
13
14
15
16
17
18
19
20
21
−3
−2
−1
0
1
2
3
4
5
6
BS
BHB
HB
RGB

7

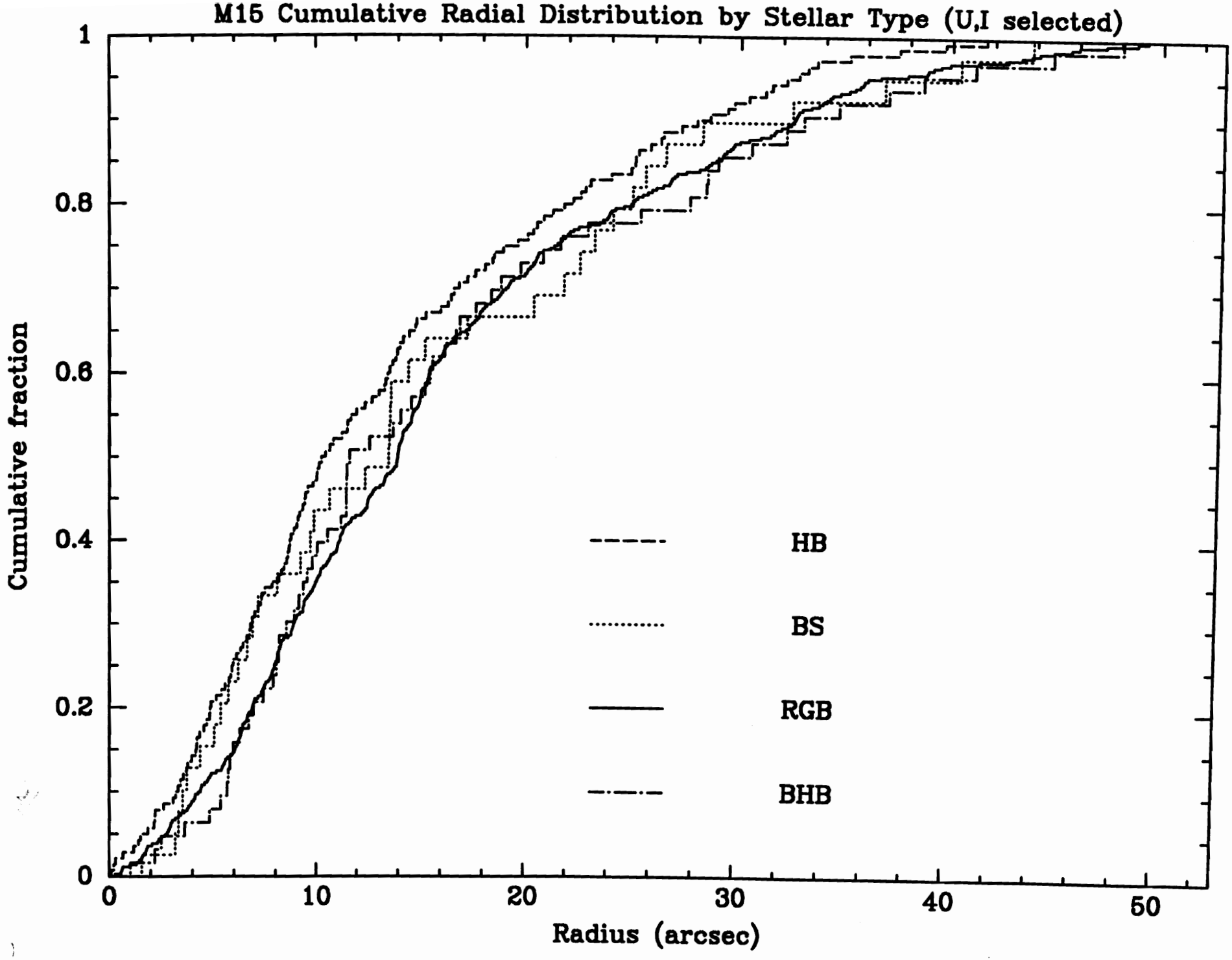
M15 Cumulative Radial Distribution by Stellar Type (U,I selected)
Cumulative fraction
Radius (arcsec)
0
0.2
0.4
0.6
0.8
1
0
10
20
30
40
50
HB
BS
RGB
BHB